


## Article

# Detection and Stability of Cyanogen Bromide and Cyanogen Iodide in Drinking Water

Fuyang Jiang<sup>1,2,3</sup>, Yuefeng Xie<sup>4</sup>, Kun Dong<sup>1,2,3,\*</sup> , Dunqiu Wang<sup>1,2,3,\*</sup> and Haixiang Li<sup>1,2,3</sup>

- <sup>1</sup> College of Environmental Science and Engineering, Guilin University of Technology, 319 Yanshan Street, Guilin 541006, China; jiangfuyang@glut.edu.cn (F.J.); lihaixiang0627@163.com (H.L.)
- <sup>2</sup> Guangxi Collaborative Innovation Center for Water Pollution Control and Safety in Karst Area, Guilin University of Technology, Guilin 541006, China
- <sup>3</sup> The Guangxi Key Laboratory of Theory and Technology for Environmental Pollution Control, Guilin 541006, China
- <sup>4</sup> School of Science, Engineering, and Technology, Pennsylvania State University, Middletown, PA 17057, USA; yxx4@psu.edu
- \* Correspondence: 2020005@glut.edu.cn (K.D.); wangdunqiu@sohu.com (D.W.)

**Abstract:** This study systematically summarized the factors affecting the stability of CNXs, providing a reference for better control and elimination of CNXs. A method for the detection of CNBr and CNI in solution was established using a liquid–liquid extraction/gas chromatography/electron capture detector. Specifically, the method was used to investigate the stability of CNBr and CNI in drinking water, especially in the presence of chlorine and sulfite, and it showed good reproducibility (relative standard deviation <3.05%), high sensitivity (method detection limit <100 ng/L), and good recovery (91.49–107.24%). Degradation kinetic studies of cyanogen halides were conducted, and their degradation rate constants were detected for their hydrolysis, chlorination, and sulfite reduction. For hydrolysis, upon increasing pH from 9.0 to 11.0, the rate constants of CNCl, CNBr, and CNI changed from 8 to  $155 \times 10^{-5} \text{ s}^{-1}$ , 1.1 to  $34.2 \times 10^{-5} \text{ s}^{-1}$ , and 1.5 to  $6.2 \times 10^{-5} \text{ s}^{-1}$ , respectively. In the presence of 1.0 mg/L chlorine, upon increasing pH from 7.0 to 10.0, the rate constants of CNCl, CNBr, and CNI changed from 36 to  $105 \times 10^{-5} \text{ s}^{-1}$ , 15.8 to  $49.0 \times 10^{-5} \text{ s}^{-1}$ , and 1.2 to  $24.2 \times 10^{-5} \text{ s}^{-1}$ , respectively. In the presence of 3  $\mu\text{mol/L}$  sulfite, CNBr and CNI degraded in two phases. In the first phase, they degraded very quickly after the addition of sulfite, whereas, in the second phase, they degraded slowly with rate constants similar to those for hydrolysis. Owing to the electron-withdrawing ability of halogen atoms and the nucleophilic ability of reactive groups such as  $\text{OH}^-$  and  $\text{ClO}^-$ , the rate constants of cyanogen halides increased with increasing pH, and they decreased in the order of  $\text{CNCl} > \text{CNBr} > \text{CNI}$  during hydrolysis and chlorination. The hydrolysis and chlorination results could be used to assess the stability of cyanogen halides in water storage and distribution systems. The sulfite reduction results indicate that quenching residual oxidants with excess sulfite could underestimate the levels of cyanogen halides, especially for CNBr and CNI.



**Citation:** Jiang, F.; Xie, Y.; Dong, K.; Wang, D.; Li, H. Detection and Stability of Cyanogen Bromide and Cyanogen Iodide in Drinking Water. *Water* **2022**, *14*, 1662. <https://doi.org/10.3390/w14101662>

Academic Editors: Yulin Tang, Shiqing Zhou and Xiaoyan Ma

Received: 1 May 2022

Accepted: 18 May 2022

Published: 23 May 2022

**Publisher's Note:** MDPI stays neutral with regard to jurisdictional claims in published maps and institutional affiliations.

**Keywords:** cyanogen bromide; cyanogen iodide; detection; stability; kinetics



**Copyright:** © 2022 by the authors. Licensee MDPI, Basel, Switzerland. This article is an open access article distributed under the terms and conditions of the Creative Commons Attribution (CC BY) license (<https://creativecommons.org/licenses/by/4.0/>).

## 1. Introduction

In the process of disinfection of drinking water, disinfectants not only kill viruses and bacteria in the water, but also react with natural organic matter to form new organic matter known as disinfection byproducts (DBPs). In recent years, nitrogenous disinfection byproducts (N-DBPs) such as dimethyl nitrosamine [1,2], halonitromethane [3,4], and halogenated nitriles [5,6] have been extensively investigated owing to their high carcinogenic and mutagenic characteristics [7,8]. Many studies have focused on the occurrence [9,10], formation [11–14], analysis [15,16], health effects [17,18], and control [19,20] of N-DBPs. In comparison with regulated trihalomethanes (THMs) and haloacetic acids (HAAs), N-DBPs exhibit higher cytotoxicity and genetic toxicity [21,22]. Muellner et al. [23] studied the

cytotoxicity and genotoxicity of seven kinds of halogenated nitriles (HANs) using the Chinese hamster ovary (CHO) cell test system and reported that the cytotoxicity of HANs is higher than that of regulated trihalomethanes and halogen acetic acid. HANs, including cyanogen halides (CNXs) and halogen acetonitriles, were also used as chemical weapon agents during the First World War [24]. The chemical dangers of these CNXs have also been reported by International Chemical Safety Cards (ICSC). Cyanogen chloride (CNCl) has been listed on the US Environmental Protection Agency (USEPA) First Acute Exposure Guideline Level (AEGL) chemical priority list since 1997, while cyanogen bromide (CNBr) and cyanogen iodide (CNI) have been listed on the Second AEGL chemical priority list since 2002. In addition, both the WHO (World Health Organization) and the Chinese Standards for Drinking Water Quality (Ministry of Health of the People's China, 2006) have established a guideline value of 70 µg/L based on cyanide for CNCl. The Agricultural Research Management Council of Australia and New Zealand has also established a guideline value for CNCl of 80 µg/L based on cyanide [25]. USEPA are established a guideline value of 200 µg/L based on cyanide for CNCl. CNBr and CNI are very toxic to aquatic organisms, and they may cause long-term adverse effects in the aquatic environment.

Photocatalysis [26], physical adsorption, biodegradation, and chemical degradation have been investigated for the removal of DBPs. Most chemical degradation studies focused on the effect of hydrolysis, chlorination, and S(IV) reduction [27,28]. Ding et al. [29] studied the effect of hydrolysis,  $[\text{OCl}^-]$ , and S(IV) reduction on the degradation of haloacetamides (HAMs) in drinking water. The results indicated that the degradation rates of HAMs increase with increasing pH. The hydrolysis and chlorination rates of HAMs increase with an increase in the number of halogens substituted on the methyl group. Owing to the decrease in the electron-withdrawing inductive effect from the chlorine to iodine atom, the reactive order of analogues is as follows: chlorinated HAMs > brominated HAMs > iodinated HAMs. The reaction of S(IV) with HAMs is mainly with respect to sulfite rather than bisulfite, and the degradation rates increase with increasing concentration of S(IV). Shang et al. [30] evaluated the kinetics of CNCl destruction using chemical reduction methods, with thiosulfate, sulfite, metabisulfite, ferrous ion, and zero-valent iron at various concentrations and pH. The CNCl destruction was primarily attributed to the chemical reduction pathway and followed second-order reaction kinetics. Among the tested compounds and pH, the S(IV) compound in the form of sulfite ( $\text{SO}_3^{2-}$ ) displayed the best destruction rate. These findings suggest that applying moderately high doses of S(IV) compounds under neutral or alkaline conditions with sufficient contact time is required for wastewater CNCl destruction. Our previous study [31] investigated the stability of CNCl in the presence of sulfite and chlorine. The results indicated that CNCl undergoes hydrolysis at high pH,  $\text{ClO}^-$  is the reactive species in chlorination oxidation, and loss of CNCl occurs in the presence of sulfite.

The standard method for the determination of CNXs is USEPA Method 524.2, which uses a purgation trap for pretreatment and gas chromatography/mass spectrometry for analysis, but it is difficult to detect CNBr due to its vapor pressure and high water solubility. Scimmenti et al. [32] compared and analyzed the advantages and disadvantages of three methods for the detection of CNCl: purge and trap–gas chromatography/mass spectrometry analysis, headspace gas chromatography/electron capture detector analysis, and micro-liquid–liquid extraction/gas chromatography/electron capture detector analysis. Cancho et al. [33] reported the simultaneous determination of CNCl and CNBr in treated water using solid-phase microextraction coupled with a gas chromatograph–electron capture detector.

CNBr and CNI in particular are tricky to analyze and typically have low analytical recoveries. A simple, rapid, and accurate method for the detection of CNBr and CNI has not been reported. Studies on the stability of CNCl can be found in the literature [27,28,30,31], but the stability of CNBr and CNI has not been reported. The objectives of this study were to establish a simple, rapid, and accurate detection method and to systematically study the kinetics and influencing factors of CNXs including hydrolysis, chlorination, and

sulfite reduction at different pH values. The results can be used to better control CNXs in drinking water distribution systems and provide data support for research on ecological and health risks.

## 2. Materials and Methods

### 2.1. Reagents

CNBr (CAS 506-68-3; MW 105.92) of guaranteed reagent purity (GR grade,  $\geq 99.8\%$ ) was purchased from Aldrich Chemical Company, Milwaukee, WI, USA; CNI (CAS 506-78-5; MW 152.92) of GR grade ( $\geq 99.8\%$ ) was purchased from City Chemical, West Haven, CT, USA; methyl *tert*-butyl ether (CAS: 1634-04-4) of high-performance liquid chromatography purity (HPLC grade,  $\geq 99.8\%$ ) was purchased from Sigma-Aldrich Company, Milwaukee, WI, USA; 1,2-dibromopropane (CAS: 78-75-1) of GR grade ( $\geq 99.8\%$ ) and chlorine of American Chemical Society standard purity (ACS grade,  $\geq 99.7\%$ ) were purchased from VWR, Philadelphia, PA, USA; most other chemicals of ACS grade ( $\geq 99.7\%$ ) for this research were purchased from Fisher Scientific, Fair Lawn, NJ, USA.

### 2.2. Sample Preparation and Analysis

Sodium dihydrogen phosphate (0.02 mol/L) and disodium hydrogen phosphate (0.02 mol/L) were prepared by adding sodium dihydrogen phosphate and disodium hydrogen phosphate into deionized water, respectively. Phosphate buffer (0.02 mol/L) at the desired pH was prepared by combining 0.02 mol/L sodium dihydrogen phosphate and 0.02 mol/L disodium hydrogen phosphate. The buffer solution was stored in a locker.

CNBr (200 mg/L) solution and CNI (200 mg/L) solution were prepared by adding CNBr and CNI into methyl *tert*-butyl ether (MTBE), respectively. CNBr and CNI solutions were stored in the fridge.

The method used for CNCl sample preparation and analysis was reported by Xie and Reckhow [31]. For CNBr and CNI analysis, as shown in Figure 1, 30 mL of sample was poured into a 40 mL amber EPA vial, and the pH of each sample was then adjusted to less than 4 with 1 M sulfuric acid. The sample was shaken by hand for 3 min after 6.0 mL of MTBE (containing 300  $\mu\text{g/L}$  1,2-dibromopropane) was added. Samples were allowed to stand for 5 min, and 1 mL of the top organic layer was transferred to a gas chromatography (GC) vial with a Pasteur pipette for sample analysis.

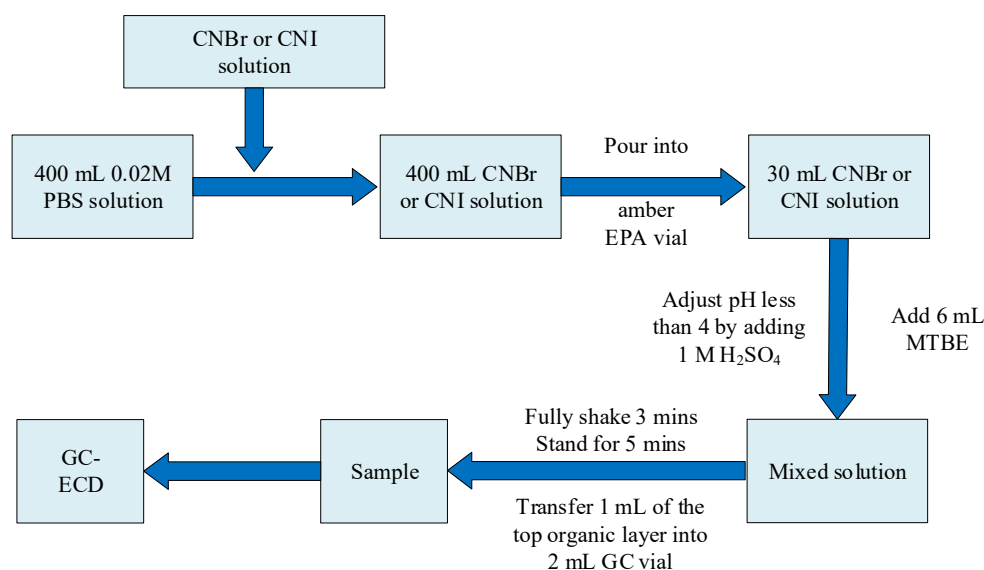


**Figure 1.** Flowchart of sample preparation.

An Agilent 6890N (Agilent Technologies, Inc., Santa Clara, CA, USA) series GC system with a micro electron capture detector (GC-ECD), HP 7683 autoinjector, HP autosampler

tray module, and Agilent DB-1701 capillary column coated with dimethylpolysiloxane (30 m × 0.25 mm × 0.25 μm) and an HP PC were employed. Data collection was accomplished using HP Chemstation software.

Nitrogen was used as the carrier gas at 3.7 mL/min. The injection temperature of the GC-ECD for CNBr and CNI was 200 °C, and splitless mode was used for injecting the 1 μL sample using the auto injector module. The ECD was operated at 300 °C with a makeup gas (nitrogen) flow rate of 60 mL/min. For CNBr, the oven temperature was programmed at 35 °C (1 min), increased to 36 °C at 0.1 °C/min (2 min) and 156 °C at 10 °C/min (2 min), and held at 200 °C (2 min). For CNI, the oven temperature was programmed at 35 °C (1 min), increased to 36 °C at 0.1 °C/min (2 min) and 136 °C at 10 °C/min (2 min), and held at 155 °C (2 min).

### 2.3. Kinetic Studies

CNXs were added into amber glass bottles with 400 mL of phosphate buffer solution, and samples were fully mixed at room temperature (1.0 mg/L chlorine was added for chlorination, and 3 μM sodium sulfite was added for sulfite reduction). The 30 mL samples were transferred into 40 mL amber EPA vials at 0, 15, 30, 60, 90, and 120 min for liquid–liquid extraction pretreatment. CNX concentrations were detected using an HP 6890 series GC system following extraction. Parallel tests were conducted simultaneously, and seven replications were carried out. The data for CNCl were obtained from Xie and Reckhow [31].

## 3. Results and Discussion

The carbon atoms in CNXs are *sp* hybridized, and the three atoms of carbon, nitrogen, and halogen are arranged in a straight line. The most critical step in the processes of CNX hydrolysis, chlorination reduction, and sulfite reduction is the dehalogenation substitution reaction. The carbon atom is attacked by a nucleophile; then, the carbon halogen bond is broken, and the halogen ions leave. The toxicity of the reaction product is greatly reduced, and no redox reaction occurs in the process. In the process of chlorination reduction, hypochlorous acid will continue to oxidize cyanate and bromine or iodide ions to generate carbon dioxide, nitrogen, and bromate or iodate.

### 3.1. Detection Method

CNBr and CNI solutions of 50 μg/L were prepared in deionized water and analyzed. The relative standard deviation (RSD), method detection limit (MDL), and recovery rate were calculated, as summarized in Table 1. For CNBr and CNI, this detection method showed good reproducibility (RSD < 3.05%), high sensitivity (MDL < 100 ng/L), and good recovery (91.49–107.24%).

**Table 1.** Relative standard deviation (RSD), method detection limit (MDL), and recovery.

Amount Added	CNBr (50 μg/L)	CNI (50 μg/L)
Amount detected (μg/L)	51.96	47.32
	49.52	49.91
	52.25	46.31
	51.75	45.90
	49.49	45.74
	47.69	46.73
	47.11	48.57
	46.73	45.76
	53.62	48.51
	52.27	48.16
RSD (%)	2.461	3.044
MDL (ng/L)	77.28	95.58
Recovery (%)	93.46–107.24	91.49–99.81

As shown in Figure 2, the calibration curves of CNI and CNBr showed a high linear relation between concentration and area ratio, indicating that this method can be used for the detection of CNI and CNBr. The main difference between this method and USEPA Method 551.1 is that this method does not use anhydrous sodium sulfate to enhance liquid–liquid extraction. Although anhydrous sodium sulfate can promote the separation of the aqueous and organic phases, impurities such as sodium sulfite can result in concentration loss by reacting with CNI and CNBr. Without anhydrous sodium sulfate, the volume of the organic phase changed from 3 mL to about 1.1 mL after extraction. To make it easier to transfer the organic phase into GC vials, the volume of added MTBE was increased from 3 mL to 6 mL.

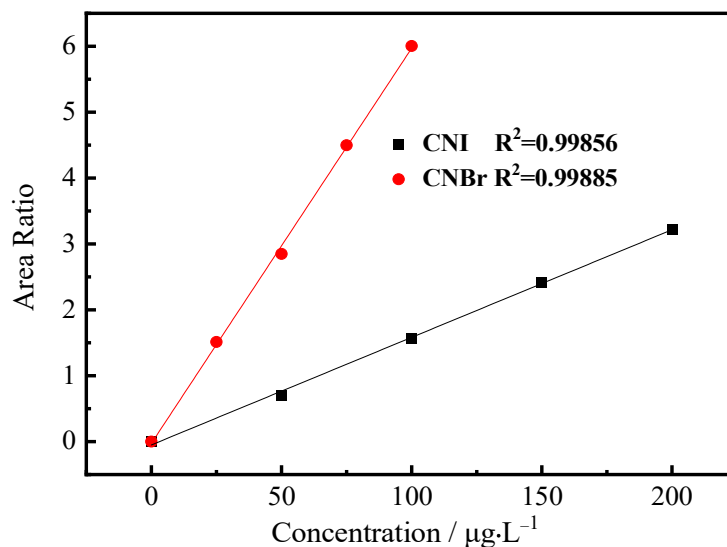


Figure 2. Calibration curves of CNI and CNBr.

### 3.2. Stability of CNXs

#### 3.2.1. Hydrolysis of CNXs

CNXs are a class of pseudohalogens, which have similar properties to halogens and can disproportionately react with water to generate cyanic acid (HCNO) and hydrogen halide (HX), as shown in Figure 3a. CNX hydrolysis in neutral and alkaline solutions is a dehalogenation reaction, as shown in Figure 3b. In acidic solutions, hydrogen ion formation and hydrolysis are inhibited, while alkaline solutions promote hydrolysis.

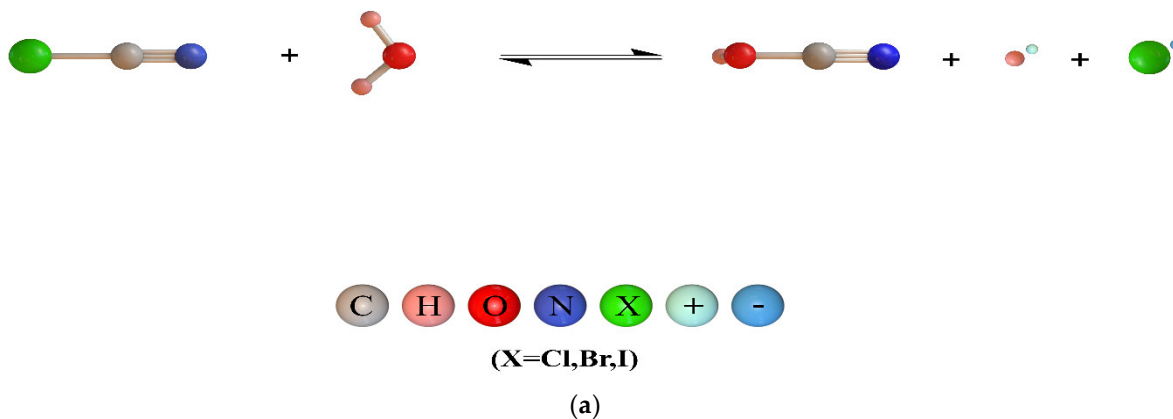
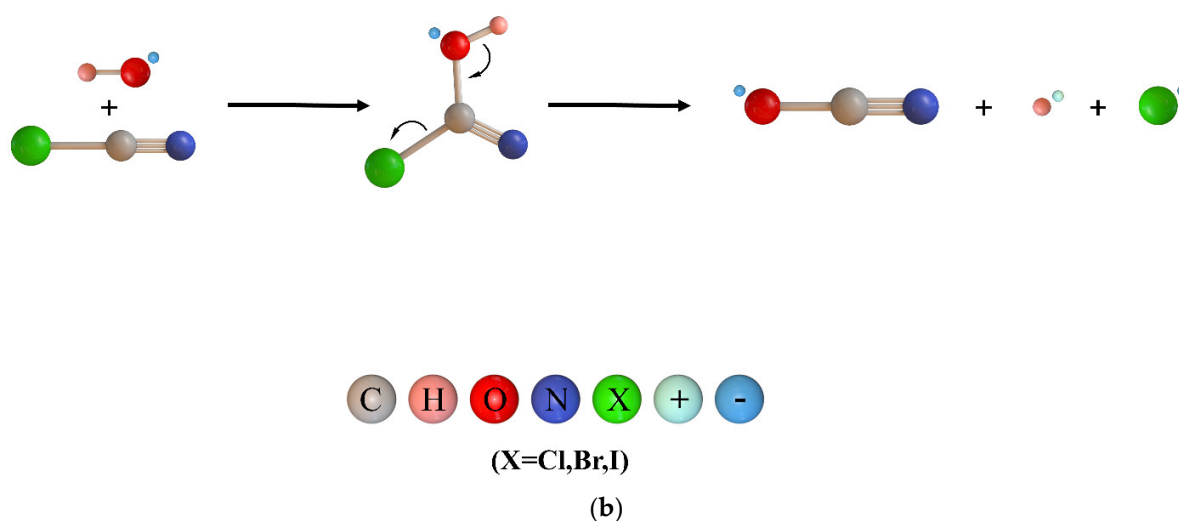


Figure 3. Cont.



**Figure 3.** Schematic of CNX hydrolysis: (a) disproportionation reaction; (b) reaction in highly alkaline solution.

Because  $[OH^-]$  does not change in phosphate-buffered solution, the hydrolysis of CNXs can be described as a pseudo-first-order reaction, as defined by Equation (1), where  $k_h$  is the pseudo-first-order hydrolysis rate constant obtained from the slope of each line. Straight lines of  $\ln(C_t/C_0)$  vs. time, as shown in Figure 4, also confirmed that these reactions are pseudo-first-order.

$$-\frac{d[CNX]}{dt} = k_h[CNX]. \quad (1)$$

The linearity of the plots, as shown in Figure 5, suggests that  $k_h$  can be expressed by Equation (2)

$$k_h = k_{OH^-}[OH^-], \quad (2)$$

where  $k_{OH^-}$  is the slope of each line. Therefore, the pH-variable hydrolysis of CNXs can be expressed by a second-order degradation reaction, as shown in Equation (3).

$$-\frac{d[CNX]}{dt} = k_h[CNX] = k_{OH^-}[CNX][OH^-]. \quad (3)$$

A common phenomenon of these three CNXs is that  $k_h$  increased with increasing pH, as shown in Table 2 and Figure 4. As the conjugate base of  $H_2O$ ,  $OH^-$  is more nucleophilic than  $H_2O$ , and it is more active than  $H_2O$  in accelerating CNX hydrolysis. As shown in Figure 5, the  $k_h$  of CNXs had a linear relationship with  $[OH^-]$ , and the three  $k_{OH^-}$  slopes decreased in the order of  $CNCl > CNBr > CNI$ . This indicates that the effect of  $OH^-$  on the stability of the CNXs decreased in the order of  $CNCl > CNBr > CNI$ .

**Table 2.** Reaction rate constants of CNXs compounds at different pH values ( $k_h$ ,  $10^{-5} s^{-1}$ ).

pH	$[OH^-]$ (mol/L)	CNCl [31]	CNBr	CNI
9.0	$10^{-5}$	$8 \pm 4$	$1.1 \pm 0.3$	$1.5 \pm 0.7$
10.0	$10^{-4}$	$27 \pm 4$	$3.7 \pm 1.2$	$3.9 \pm 0.7$
11.0	$10^{-3}$	$155 \pm 5$	$34.2 \pm 2$	$6.2 \pm 1.4$

As the electron-withdrawing ability follows the order of Cl (Pauling electronegativity 3.16) > Br (Pauling electronegativity 2.96) > I (Pauling electronegativity 2.66), the electronic cloud density of the carbon ion (the ability of a carbon atom to accept lone pair electrons) is  $CNI > CNBr > CNCl$ . This indicates that the order of these compounds being attacked by nucleophiles is  $CNCl > CNBr > CNI$ . However, the bond length order of C–X is C–I > C–Br > C–Cl, and the bond energy order of C–X is C–Cl > C–Br > C–I, indicating that

the dehalogenation order is CNI > CNBr > CNCl. The pseudo-first-order hydrolysis rate constants shown in Table 2 indicate that the electron-withdrawing ability of halogen atoms was the major factor influencing the hydrolysis of these compounds at the same pH.

In acidic and neutral solutions, the hydrolysis of CNXs is inhibited, and a lower pH results in more obvious inhibition, while the  $k_h$  of CNX compounds is so low that it can be ignored [31]. In alkaline solutions, the  $k_h$  of CNX compounds is affected by the  $[OH^-]$  and the electron density cloud of the carbon ion. A higher pH results in a higher  $k_h$  of the CNXs. At the same pH, the order of the  $k_h$  is CNCl > CNBr > CNI. The hydrolysis can have an effect on the stability of CNXs, especially with a stronger electron-withdrawing property and at higher pH.

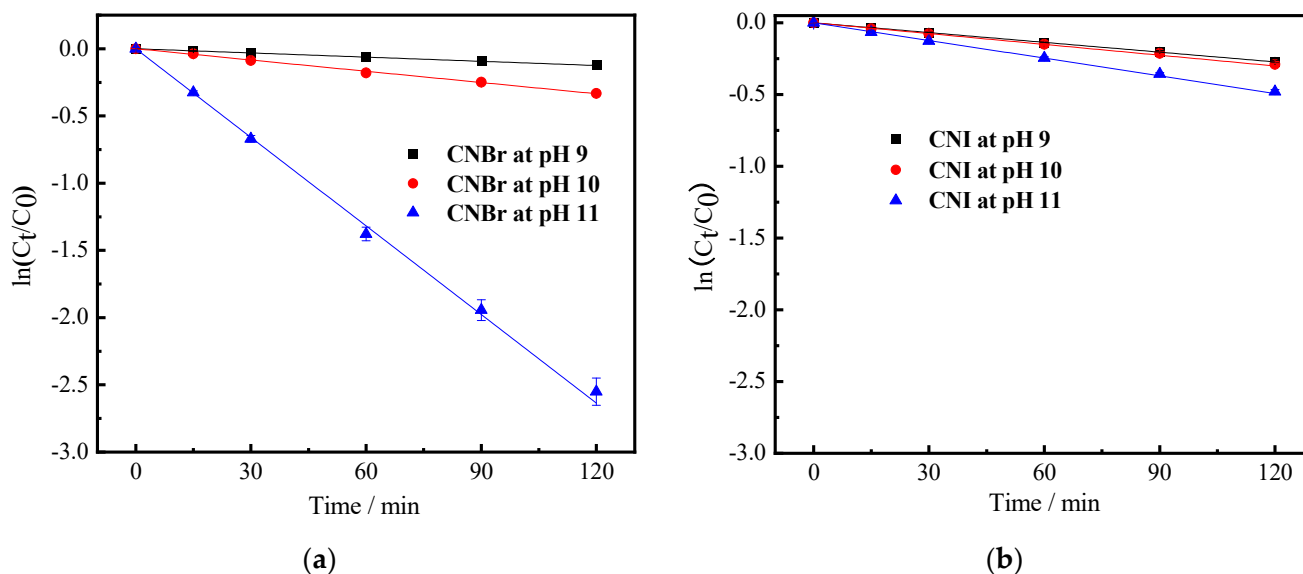


**Figure 4.** Hydrolysis of CNBr (a) and CNI (b) at different pH values ( $[CNBr]_0 = 100 \mu\text{g/L}$ ,  $[CNI]_0 = 150 \mu\text{g/L}$ ).

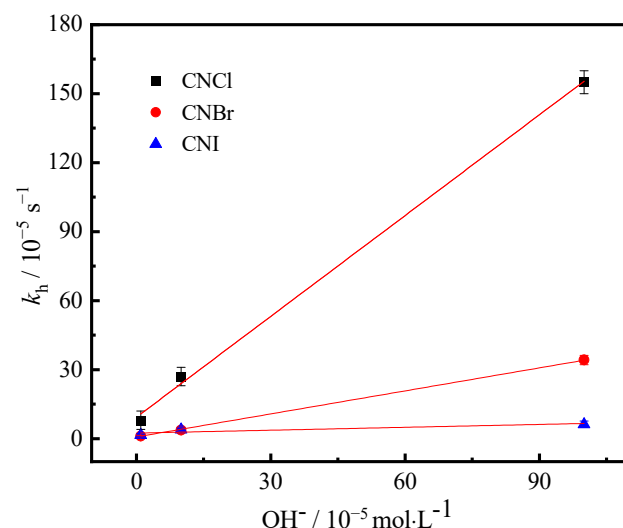


**Figure 5.** CNXs hydrolysis rate as a function of  $[OH^-]$ .

### 3.2.2. Chlorination of CNXs

The chlorination of CNXs involves a reaction between CNXs and hypochlorous acid and hypochlorite. The rate constant obtained in the reduction process ( $k_{obs}$ ) contains both the hydrolysis rate constant ( $k_h$ ) and chlorination rate constant ( $k_{Cl_2}$ ). The chlorination of

CNXs can also be described as a pseudo-first-order reaction, as defined by Equation (4), according to the straight lines shown in Figure 6.

$$-\frac{d[\text{CNX}]}{dt} = k_{\text{Cl}_2}[\text{CNX}]. \quad (4)$$

Both  $[\text{HClO}]$  and  $[\text{ClO}^-]$  affect the chlorination rate constant  $k_{\text{Cl}_2}$  as shown in Equation (5).

$$k_{\text{Cl}_2} = k_{\text{ClO}^-}[\text{ClO}^-] + k_{\text{HClO}}[\text{HClO}]. \quad (5)$$

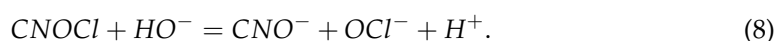
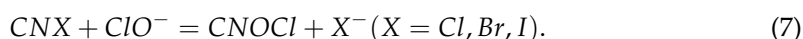
As shown in Table 3, at pH 5.0,  $[\text{ClO}^-]$  was  $4.18 \times 10^{-8}$  M, and the  $k_{\text{Cl}_2}$  of the CNXs was lower than  $1 \times 10^{-5} \text{ s}^{-1}$ ; at pH 10.0,  $[\text{ClO}^-]$  was  $1.41 \times 10^{-5}$  M, and the  $k_{\text{Cl}_2}$  of CNCl, CNBr, and CNI was  $105 \times 10^{-5} \text{ s}^{-1}$ ,  $45.3 \times 10^{-5} \text{ s}^{-1}$ , and  $20.9 \times 10^{-5} \text{ s}^{-1}$ , respectively. These values indicate that  $[\text{ClO}^-]$  was the major factor in CNX chlorination.

The parameter  $\alpha_{\text{ClO}^-}$  is defined as the fraction of chlorine present as  $\text{ClO}^-$  and is calculated using Equation (6) with a HClO dissociation constant  $K_a$  of  $2.98 \times 10^{-8}$  M at room temperature.

$$\alpha_{\text{ClO}^-} = \frac{[\text{ClO}^-]}{[\text{Cl}]_T} = \frac{[\text{ClO}^-]}{[\text{ClO}^-] + [\text{HClO}]} = \frac{K_a}{K_a + [\text{H}^+]}. \quad (6)$$

As shown in Table 3 and Figure 6, high pH promoted the reduction of CNXs. A higher pH resulted in a higher  $\alpha_{\text{ClO}^-}$  and  $[\text{OH}^-]$ , as well as a larger  $k_{\text{Cl}_2}$ . The large difference in  $k_{\text{Cl}_2}$  at  $\alpha_{\text{ClO}^-}$  of 0.3% and 99.7% indicates that  $\alpha_{\text{ClO}^-}$  was the major factor influencing CNX stability with chlorine.

The reaction between hypochlorite and CNXs is a complex process [34], and the reaction can be simplified as shown in Equation (7). Because hypochlorous acid is more acidic than  $\text{H}_2\text{O}$ , the corresponding conjugate base  $\text{ClO}^-$  is less nucleophilic than  $\text{HO}^-$ . Therefore,  $\text{HO}^-$  can react with  $\text{CNOCl}$  to form  $\text{ClO}^-$ , which acts as a catalyst in the reaction [26], as shown in Equations (7) and (8).



As shown in Table 3 and Figure 7,  $[\text{OH}^-]$ ,  $[\text{ClO}^-]$ , and  $\alpha_{\text{ClO}^-}$  increased with increasing pH. The  $k_{\text{Cl}_2}$  order of the CNXs was  $\text{CNCl} > \text{CNBr} > \text{CNI}$  at the same pH, and the  $k_{\text{Cl}_2}$  values increased with increasing pH. The results of CNXs chlorination were similar to the hydrolysis results.

CNX chlorination is actually caused by hypochlorite, which works as a catalyst to promote the hydrolysis of CNXs. These results can also explain why CNXs are rarely detected in water with chlorine residue.

**Table 3.** Reaction rate constants for CNXs at different pH values in the presence of chlorine ( $k_{\text{Cl}_2}$ ,  $10^{-5} \text{ s}^{-1}$ ).

pH	$[\text{OH}^-]$ (mol/L)	$\alpha_{\text{ClO}^-}$ (%)	$[\text{ClO}^-]$ (mol/L)	CNCl [31]	CNBr	CNI
5.0	$10^{-9}$	0.3	$4.18 \times 10^{-8}$	–	$0.9 \pm 0.5$	$0.8 \pm 0.5$
7.0	$10^{-7}$	23.0	$3.24 \times 10^{-6}$	$36 \pm 2$	$15.8 \pm 1.9$	$1.2 \pm 0.9$
9.0	$10^{-5}$	96.8	$1.36 \times 10^{-5}$	$91 \pm 5$	$39.3 \pm 2.5$	$6.7 \pm 0.8$
10.0	$10^{-4}$	99.7	$1.41 \times 10^{-5}$	$105 \pm 10$	$45.3 \pm 4.3$	$20.9 \pm 4.5$



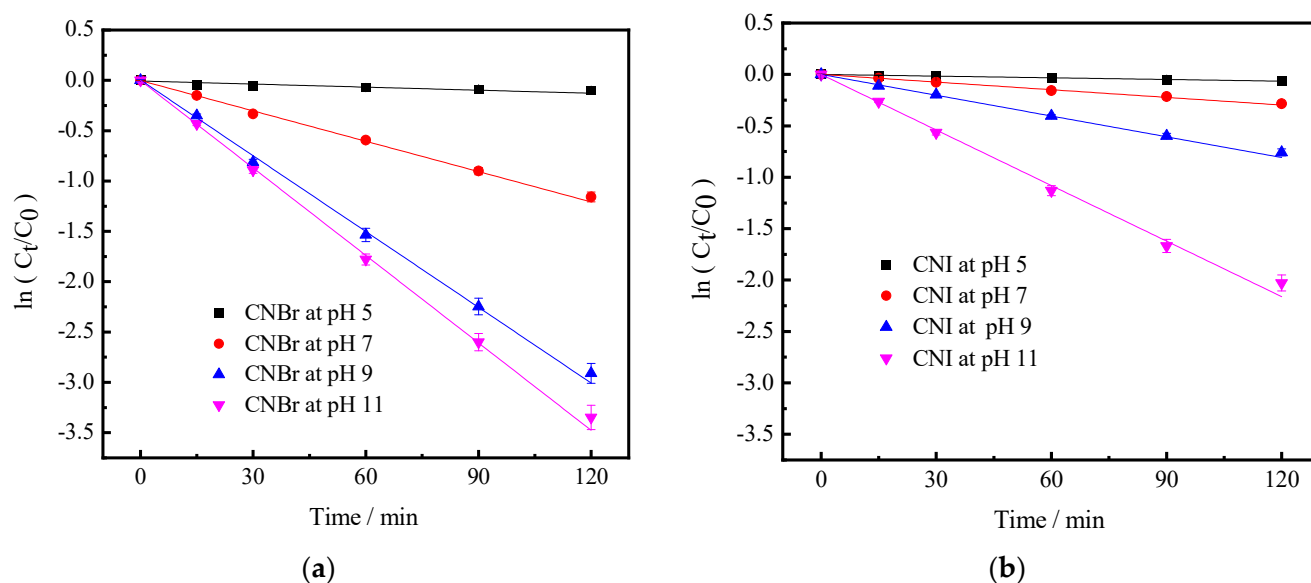


**Figure 6.** Stability of CNBr (a) and CNI (b) in the presence of chlorine ( $[CNBr]_0 = 100 \mu\text{g/L}$ ,  $[CNI]_0 = 150 \mu\text{g/L}$ ,  $[Cl_2]_0 = 1.0 \text{ mg/L}$ ).

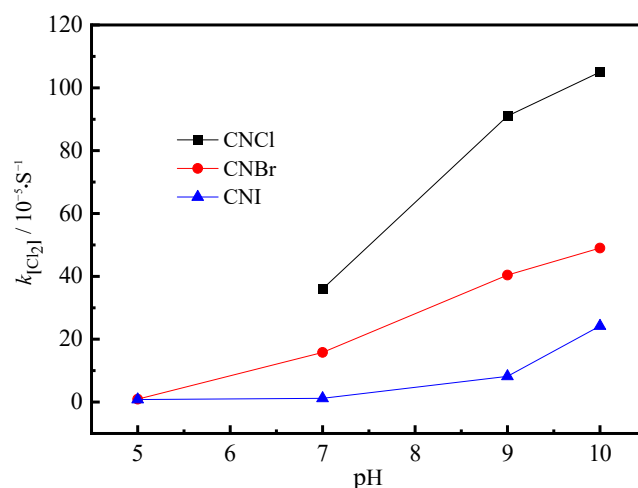


**Figure 7.** Effect of pH on the stability of CNXs.

### 3.2.3. Sulfite Reduction of CNBr and CNI

As shown in Table 4 and Figure 8, high pH promotes CNBr and CNI degradation reactions. A higher pH resulted in a larger sulfite reduction rate constant  $k_s$ . Owing to the increasing bond length and decreasing dissociation energies of C–X, the tendency for halogen substituents to be attacked by ionic or radical reductants [35] follows the order of  $I > Br > Cl$ . The electronic cloud density of CN follows the order of  $CNI > CNBr > CNCl$ , which indicates that the order in which the compounds are attacked by nucleophiles is  $CNCl > CNBr > CNI$ . The order of the reaction rate constants for CNXs at the same pH is  $CNI > CNBr > CNCl$ . The results indicate that the bond energy of C–X was the major factor in the sulfite reduction of these compounds at the same pH.

**Table 4.** Reaction rate constants for CNXs at different pH values in the presence of sulfite ( $k_s, 10^{-5} \text{ s}^{-1}$ ).

pH	$\alpha_{\text{SO}_3^{2-}}$	CNBr	CNI
5.0	0.66%	>1460	>1620
7.0	39.76%	>1515	>1715
9.0	98.51%	>1680	>2200

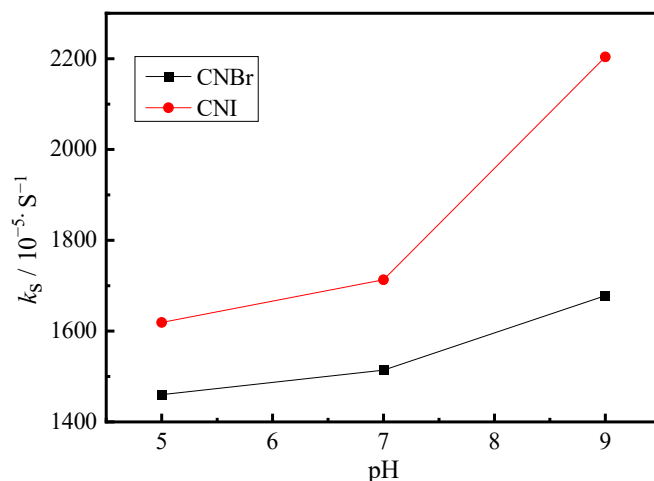


**Figure 8.** Effect of pH on the stability of CNBr and CNI.

Bailey and Bishop [36] reported that the reaction between CNCl and sulfite may produce S–N–O ring-structured compounds, which could reproduce sulfite ions with cyanate and chloride. Throughout the reaction process, there is no redox reaction, and the sulfite acts as a catalyst to promote the reaction of water molecules or hydroxide with CNCl to remove chloride ions. Shang et al. [30] also observed similar phenomena and suggested that the reaction between sulfite and CNCl may form sulfate, chloride, cyanate, and other products. From the perspective of the products, the presence of chloride ions and cyanate indicates that CNCl does not participate in the redox reaction, and it may be the dissolved oxygen in the solution that oxidizes sulfite to sulfate.

Xie and Reckhow [31] reported that the degradation of CNCl is a pseudo-first-order reaction. Because the hydrolysis rate is negligible at pH 8.2 or below compared to the sulfite reduction rate, the pseudo-first-order reaction can be expressed by Equation (9).

$$-\frac{d[\text{CNCl}]}{dt} = k_s[\text{CNCl}]. \quad (9)$$

Because  $[\text{H}_2\text{SO}_3]$  is negligible above pH 4,  $k_s$  can be expressed by Equation (10).

$$k_s = k_{\text{HSO}_3^-}[\text{HSO}_3^-] + k_{\text{SO}_3^{2-}}[\text{SO}_3^{2-}]. \quad (10)$$

Xie and Reckhow [31] proposed that, compared to the  $k_{\text{SO}_3^{2-}}$  of  $11.3 \text{ M}^{-1} \cdot \text{s}^{-1}$ , the  $k_{\text{HSO}_3^-}$  of  $0.55 \text{ M}^{-1} \cdot \text{s}^{-1}$  is negligible. The results indicate that  $[\text{SO}_3^{2-}]$  was the major factor in the sulfite reduction of CNXs.

The parameter  $\alpha_{\text{SO}_3^{2-}}$  is defined as the fraction of sulfite present as  $\text{SO}_3^{2-}$  and is calculated using Equation (11).

$$\alpha_{\text{SO}_3^{2-}} = \frac{[\text{SO}_3^{2-}]}{[\text{S(IV)}]_T} = \frac{K_{a1}K_{a2}}{K_{a1}K_{a2} + K_{a1}[\text{H}^+] + [\text{H}^+]^2}. \quad (11)$$

Sulfites and bisulfites are the dominant forms of S(IV) in the pH range of 5 to 9. As shown in Table 4, the  $k_s$  of the CNXs increased with increasing  $\alpha_{\text{SO}_3^{2-}}$ . A higher  $\alpha_{\text{SO}_3^{2-}}$  resulted in a larger  $k_s$ . This indicates that sulfite plays a greater role than bisulfite in the stability of CNXs with sodium sulfite. The effect of pH on CNX degradation is in the order of CNI > CNBr. This is explained by the fact that the electron-withdrawing property of the halogens is Cl > Br > I and the bond energy of C–X is C–Cl > C–Br > C–I; thus, the order of forming  $\text{CN}^+$  and converting to  $\text{CN}^-$  is CNI > CNBr > CNCl.

In the presence of sulfite, sulfite ion is the main factor affecting the degradation process of CNCl, and its effect is much greater than that of sulfite ion; the degradation of CNI and

CNBr is affected by the combined action of sulfite ion and bisulfite ion, and, although the influence of sulfite ion is relatively greater, the effects of both ions cannot be ignored.

As shown in Figure 9, the concentrations of CNBr and CNI decreased sharply in the first few minutes of the reaction, and then their degradation became gradual, similar to their hydrolysis degradation. The sharp decrease in the CNBr and CNI concentration in the first few minutes of the reaction was the main cause of the observed concentration loss and low recovery rate in the detection process.

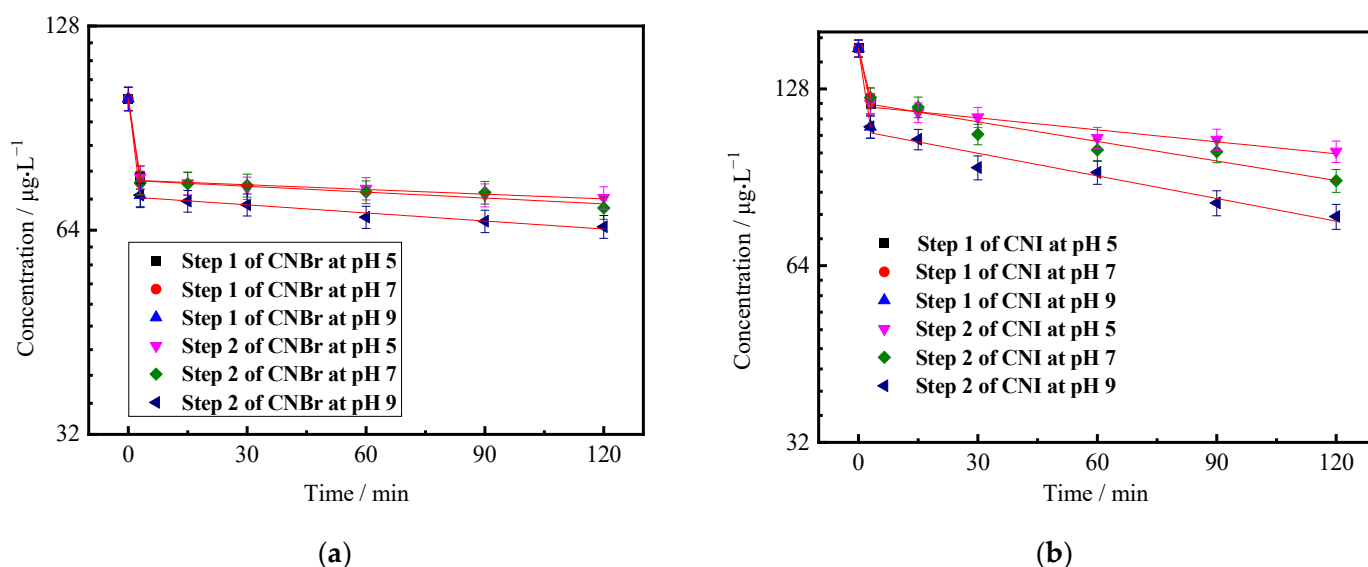


**Figure 9.** Stability of CNBr (a) and CNI (b) in the presence of sulfite ( $[\text{CNBr}]_0 = 100 \mu\text{g/L}$ ,  $[\text{CNI}]_0 = 150 \mu\text{g/L}$ ,  $[\text{SO}_3^{2-}]_0 = 3 \mu\text{mol/L}$ ).

Li et al. [37,38] reported that hydrated electrons generated in the sulfite/UV process induce the dehalogenation of halogenated organic compounds. It was found that about 90% of 50  $\mu\text{M}$  monochloroacetic acid (MCAA) was degraded in 10 min (0.2 mM sulfite, pH 9.2, 25  $^\circ\text{C}$ , and oxygen-free). Because the order of Pauling electronegativity is  $\text{N} > \text{Br} > \text{I} > \text{C} > \text{H}$ , the order of carbon electronic cloud density and of compounds attacked by nucleophiles is  $\text{CNXs} > \text{MCAA}$ . The order of the steric hinderance effect also indicates that the order of dehalogenation reactivity is  $\text{CNXs} > \text{MCAA}$ . Thus, this may explain why about 30% of 1  $\mu\text{M}$  CNBr and CNI degraded in a few minutes (3  $\mu\text{M}$  sulfite, pH 9).

The rate constant,  $k_s$ , increased with increasing pH, and it increased from chloride to iodide at the same pH. These sulfite reduction results show that sulfite can result in a loss of CNXs during CNX sample preparation and analysis when sulfite is used to quench the residue of chlorine or other oxidants.

Hydrolysis is the most basic degradation mode of CNXs. Chlorination can be regarded as hydrolysis in the presence of  $\text{ClO}^-$ , which works as a catalyst. Both sulfite and bisulfite can react with CNBr and CNI, and the concentrations of CNBr and CNI decrease sharply in the first few minutes. Thus, the effect on the stability of CNBr and CNI is in the order of sulfite reduction  $>$  chlorination  $>$  hydrolysis, with  $k_s > k_{\text{Cl}_2} > k_h$  at the same pH.

#### 4. Conclusions and Future Perspectives

In this study, the detection and stability of CNXs in the presence of chlorine and sulfite were investigated. The main conclusions are as follows:

1. The detection method proposed in this study is suitable for the detection of CNBr and CNI. This method is simple (easy to operate), rapid (preparation is about 10 min, and analysis is about 34 min), and accurate (RSD  $<$  3.05%, MDL  $<$  100 ng/L, and recovery 91.49–107.24%).

2. The main factor affecting hydrolysis is  $\text{OH}^-$ . The hydrolysis rate constants,  $k_h$ , of the CNXs increase with increasing  $\text{OH}^-$  concentration, which in turn increases with increasing pH. At the same pH,  $k_h$  follows the order of  $\text{CNCl} > \text{CNBr} > \text{CNI}$ .
3. The main factor affecting chlorination reduction is  $\text{ClO}^-$  which works as a catalytic group. The chlorination rate constants,  $k_{\text{Cl}_2}$ , of the CNXs increase with increasing pH and follow the order of  $\text{CNCl} > \text{CNBr} > \text{CNI}$  at the same pH, similar to hydrolysis.
4. Both sulfite and bisulfite are factors affecting sulfite reduction. Sulfite plays a greater role than bisulfite in the stability of CNXs with sodium sulfite. Sulfite can react with CNBr and CNI rapidly. The sulfite reduction rate constants,  $k_s$ , of the CNXs increase with increasing pH and follow the order of  $\text{CNI} > \text{CNBr} > \text{CNCl}$  at the same pH.
5. Both sulfite reduction and chlorination were effective methods for the reduction of CNBr and CNI during water treatment. The effect on the stability of CNBr and CNI is in the order of sulfite reduction  $>$  chlorination  $>$  hydrolysis (at pH 9,  $k_s$  is greater than  $1680 \times 10^{-5} \text{ s}^{-1}$ ,  $k_{\text{Cl}_2}$  is between 6.7 and  $39.3 \times 10^{-5} \text{ s}^{-1}$ , and  $k_h$  is about  $1.0 \times 10^{-5} \text{ s}^{-1}$ ).

This simple and rapid detection method can provide technical support for future research. The factors and mechanisms affecting the stability of CNXs were studied. The results can provide data support for future research on CNX control, elimination, ecological risk, and health risk in drinking water.

**Author Contributions:** Conceptualization, K.D. and F.J.; methodology, Y.X.; formal analysis, F.J. and K.D.; investigation, D.W., F.J., K.D. and Y.X.; resources, D.W.; data curation, D.W., K.D., F.J. and Y.X.; writing—original draft preparation, K.D. and F.J.; writing—review and editing, K.D. and Y.X.; visualization, D.W. and F.J.; supervision, D.W. and Y.X.; project administration, K.D. and D.W.; funding acquisition, F.J. and H.L. All authors have read and agreed to the published version of the manuscript.

**Funding:** This research was funded by the Guangxi Natural Science Foundation (grant number 2022GXNSFFA035033), the National Natural Science Foundation of China (grant number 51638006), the Basic Ability Enhancement Program for Young and Middle-aged Teachers of Guangxi (grant numbers 2021KY0265 and 2017KY0269), and the Innovation Project of Guangxi Graduate Education (YCBZ2022117).

**Institutional Review Board Statement:** Not applicable.

**Informed Consent Statement:** Not applicable.

**Data Availability Statement:** The data that support the findings of this study are available from the corresponding author upon reasonable request.

**Conflicts of Interest:** The authors declare no conflict of interest.

## References

1. Zhang, B.; Liu, J.; Zhao, R.S.; Xian, Q. NDMA adsorption and degradation by a new-type of Ag-MONT material carrying nanoscale zero-valent iron. *Chemosphere* **2021**, *268*, 129271. [[CrossRef](#)]
2. Zeng, T.; Mitch, W.A. Impact of Nitrification on the Formation of N-Nitrosamines and Halogenated Disinfection Byproducts within Distribution System Storage Facilities. *Environ. Sci. Technol.* **2016**, *50*, 2964–2973. [[CrossRef](#)]
3. Shi, J.L.; Plata, S.L.; Kleimans, M.; Childress, A.E.; Mccurry, D.L. Formation and Fate of Nitromethane in Ozone-Based Water Reuse Processes. *Environ. Sci. Technol.* **2021**, *55*, 6281–6289. [[CrossRef](#)]
4. Ersan, M.S.; Ladner, D.A.; Karanfil, T. The control of N-nitrosodimethylamine, Halonitromethane, and Trihalomethane precursors by Nanofiltration. *Water Res.* **2016**, *105*, 274–281. [[CrossRef](#)]
5. Linge, K.L.; Kristiana, I.; Liew, D.; Holman, A.; Joll, C.A. Halogenated semivolatile acetonitriles as chloramination disinfection by-products in water treatment: A new formation pathway from activated aromatic compounds. *Environ. Sci. Processes Impacts* **2020**, *22*, 653–662. [[CrossRef](#)]
6. Rougé, V.; Gunten, U.V.; Allard, S. Efficiency of pre-oxidation of natural organic matter for the mitigation of disinfection byproducts: Electron donating capacity and UV absorbance as surrogate parameters. *Water Res.* **2020**, *187*, 116418. [[CrossRef](#)]
7. Rougé, V.; Shin, J.; Nguyen, P.T.T.H.; Jang, D.; Lee, W.; Escher, B.I.; Lee, Y. Nitriles as main products from the oxidation of primary amines by Ferrate(VI): Kinetics, mechanisms and toxicological implications for nitrogenous disinfection byproduct control. *Water Res.* **2022**, *209*, 117881. [[CrossRef](#)]

8. Ding, X.; Zhu, J.; Zhang, J.; Dong, T.; Xia, Y.; Jiao, J.; Wang, X.; Zhou, W. Developmental toxicity of disinfection by-product monohaloacetamides in embryo-larval stage of zebrafish. *Ecotoxicol. Environ. Saf.* **2020**, *189*, 110037. [[CrossRef](#)]
9. Yin, J.; Wu, B.; Zhang, X.X.; Xian, Q. Comparative toxicity of chloro- and bromo-nitromethanes in mice based on a metabolomic method. *Chemosphere* **2017**, *185*, 20–28. [[CrossRef](#)]
10. Tan, Y.; Lin, T.; Jiang, F.; Dong, J.; Chen, W.; Zhou, D. The shadow of dichloroacetonitrile (DCAN), a typical nitrogenous disinfection by-product (N-DBP), in the waterworks and its backwash water reuse. *Chemosphere* **2017**, *181*, 569–578. [[CrossRef](#)]
11. Tang, H.; Zhong, H.; Pan, Y.; Zhou, Q.; Xu, B. A New Group of Heterocyclic Nitrogenous Disinfection Byproducts (DBPs) in Drinking Water: Role of Extraction pH in Unknown DBP Exploration. *Environ. Sci. Technol.* **2021**, *55*, 6764–6772. [[CrossRef](#)]
12. Karanfil, T.; Krasner, S.W.; Westerhoff, P.; Xie, Y. Disinfection by-products in drinking water: Occurrence, formation, health effects, and control. *Anal. Chem.* **2000**, *72*, 26–32.
13. Wu, Y.; Sheng, D.; Wu, Y.; Sun, J.; Bu, L.; Zhu, S.; Zhou, S. Molecular insights into formation of nitrogenous disinfection byproducts from algal organic matter in UV-LEDs/chlorine process based on FT-ICR analysis. *Sci. Total Environ.* **2022**, *812*, 152457. [[CrossRef](#)]
14. Hu, J.; Xu, Y.; Chen, Y.; Chen, J.; Dong, H.; Yu, J.; Qiang, Z.; Qu, J.; Chen, J. Formation of carbonaceous and nitrogenous iodinated disinfection byproducts from biofilm extracellular polymeric substances by the oxidation of iodide-containing waters with lead dioxide. *Water Res.* **2020**, *188*, 116551. [[CrossRef](#)]
15. Li, X.; Rao, N.; Linge, K.L.; Joll, C.A.; Khan, S.; Henderson, R.K. Formation of algal-derived nitrogenous disinfection by-products during chlorination and chloramination. *Water Res.* **2020**, *183*, 116047. [[CrossRef](#)]
16. Qian, Y.; Chen, Y.; Hu, Y.; Hanigan, D.; Westerhoff, P.; An, D. Formation and control of C- and N-DBPs during disinfection of filter backwash and sedimentation sludge water in drinking water treatment. *Water Res.* **2021**, *194*, 116964. [[CrossRef](#)]
17. Ding, S.; Chu, W. Recent advances in the analysis of nitrogenous disinfection by-products. *Trends Environ. Anal. Chem.* **2017**, *14*, 19–27. [[CrossRef](#)]
18. Ashworth, I.W.; Dirat, O.; Teasdale, A.; Whiting, M. Potential for the Formation of N-Nitrosamines during the Manufacture of Active Pharmaceutical Ingredients: An Assessment of the Risk Posed by Trace Nitrite in Water. *Org. Process Res. Dev.* **2020**, *24*, 1629–1646. [[CrossRef](#)]
19. Cuthbertson, A.A.; Kimura, S.Y.; Liberatore, H.K.; Summers, R.S.; Knappe, D.R.U.; Stanford, B.D.; Maness, J.C.; Mulhern, R.E.; Selbes, M.; Richardson, S.D. Does GAC with Chlorination Produce Safer Drinking Water? From DBPs and TOX to Calculated Toxicity. *Environ. Sci. Technol.* **2019**, *53*, 5987–5999. [[CrossRef](#)]
20. Liu, C.; Olivares, C.I.; Pinto, A.J.; Lauderdale, C.V.; Brown, J.; Selbes, M.; Karanfil, T. The control of disinfection byproducts and their precursors in biologically active filtration processes. *Water Res.* **2017**, *124*, 630–653. [[CrossRef](#)]
21. Zhang, S.; Lin, T.; Chen, H.; Xu, H.; Chen, W.; Tao, H. Precursors of typical nitrogenous disinfection byproducts: Characteristics, removal, and toxicity formation potential. *Sci. Total Environ.* **2020**, *742*, 140566. [[CrossRef](#)]
22. Jaichuedee, J.; Wattanachira, S.; Musikavong, C. Kinetics of the formation and degradation of carbonaceous and nitrogenous disinfection by-products in Bangkok and Songkhla source waters. *Sci. Total Environ.* **2020**, *703*, 134888. [[CrossRef](#)]
23. Muellner, M.; Wagner, E.; Mccalla, K.; Richardson, S.; Woo, Y.; Plewa, M. Haloacetonitriles vs. regulated haloacetic acids: Are nitrogen-containing DBPs more toxic? *Environ. Sci. Technol.* **2007**, *41*, 645–651. [[CrossRef](#)]
24. Sartori, M.; Marrison, L.W. The war gases: Chemistry and analysis. *War Gases Chem. Anal.* **1939**, *118*, e19.
25. Simpson, K.L.; Hayes, K.P. Drinking water disinfection by-products: An Australian perspective. *Water Res.* **1998**, *32*, 1522–1528. [[CrossRef](#)]
26. Yaqoob, A.A.; Ahmad, H.; Parveen, T.; Ahmad, A.; Owais, M.; Ismail, I.M.I.; Huda, A.Q.; Umar, K.; Ibrahim, M.N.M. Recent Advances in Metal Decorated Nanomaterials and Their Various Biological Applications: A Review. *Front. Chem.* **2020**, *8*, 341. [[CrossRef](#)]
27. Na, C.; Olson, T.M. Stability of Cyanogen Chloride in the Presence of Free Chlorine and Monochloramine. *Environ. Sci. Technol.* **2004**, *38*, 6037–6043. [[CrossRef](#)]
28. Erik, J.P.; Mariñas, B.J. The hydroxide-assisted hydrolysis of cyanogen chloride in aqueous solution. *Water Res.* **2001**, *35*, 643–648.
29. Ding, S.; Wang, F.; Chu, W.; Cao, Z.; Pan, Y.; Gao, N. Rapid degradation of brominated and iodinated haloacetamides with sulfite in drinking water: Degradation kinetics and mechanisms. *Water Res.* **2018**, *143*, 325–333. [[CrossRef](#)]
30. Shang, C.; Qi, Y.; Xie, L.; Wei, L.; Yang, X. Kinetics of cyanogen chloride destruction by chemical reduction methods. *Water Res.* **2005**, *39*, 2114–2124. [[CrossRef](#)]
31. Xie, Y.F.; Reckhow, D.A. Stability of Cyanogen chloride in the Presence of Sulfite and Chlorine. In Proceedings of the American Water Works Association Proceedings 1992 Water Quality Technology Conference, Denver, CO, USA, 15–19 November 1992.
32. Scilimenti, M.J.; Hwang, C.J.; Krasner, S.W. A Comparison of Analytical Techniques for Determining Cyanogen Chloride in Chloraminated Drinking Water. In Proceedings of the Acs Symposium Series, Washington DC, USA, 15–19 November 1992.
33. Cancho, B.; Ventura, F.; Galceran, Z.M. Simultaneous determination of cyanogen chloride and cyanogen bromide in treated water at sub-mg/L levels by a new solid-phase microextraction-gas chromatographic-electron-capture detection method. *J. Chromatogr. A* **2000**, *897*, 307–315. [[CrossRef](#)]
34. Eden, G.E.; Hampson, B.L.; Wheatland, A.B. Destruction of cyanide in waste waters by chlorination. *J. Chem. Technol. Biotechnol.* **2010**, *69*, 244–249. [[CrossRef](#)]
35. Bauman, L.; Stenstrom, M.K. Observations of the reaction between organohalides and sulfite. *Environ. Sci. Technol.* **1989**, *23*, 232–236. [[CrossRef](#)]

36. Bailey, P.L.; Bishop, E. Hydrolysis of cyanogen chloride. *J. Chem. Soc. Dalton Trans.* **1973**, *9*, 912. [[CrossRef](#)]
37. Li, X.; Ma, J.; Liu, G.; Fang, J.; Yue, S.; Guan, Y.; Chen, L.; Liu, X. Efficient Reductive Dechlorination of Monochloroacetic Acid by Sulfite/UV Process. *Environ. Sci. Technol.* **2012**, *46*, 7342–7349. [[CrossRef](#)]
38. Li, X.; Fang, J.; Liu, G.; Zhang, S.; Pan, B.; Ma, J. Kinetics and efficiency of the hydrated electron-induced dehalogenation by the sulfite/UV process. *Water Res.* **2014**, *62*, 220–228. [[CrossRef](#)]